Impact of spatial and spectral resolutions on the classification of urban areas

Rosa Oltra-Carrio, Xavier Briottet, Marion Bonhomme

Impact of spatial and spectral resolutions on the classification of urban areas

R. Oltra-Carrió, X. Briottet and M. Bonhomme

***Abstract*— Classification of land cover in urban areas can play an important role in urban planning decisions and in characterizing urban materials properties such as reflectance. Taking into account the large offer of new and future remote sensing sensors with different spectral and spatial characteristics, it is important to compare their classification performances in urban area. To this aim, this work simulates from airborne data the at sensor images acquired bythree space borne instruments (Pléiades, SENTINEL-2 and HYPXIM) in the Visible Near Infrared (0.4 µm – 1.0 µm) and Shortwave Infrared (1.0 µm-2.5µm) spectral ranges. Five classification maps with 8 land cover classes over the city of Toulouse (France) are generated with a Support Vector Machine rule. Correct values of accuracy are obtained in all cases (kappa coefficient higher than 0.65 and overall accuracy better than 70 %). Nevertheless, coarser spatial resolutions do not allow mapping urban details and SWIR data was necessary to discriminate between classes.**

***Index Terms*—PLEIADES, SENTINEL2, Support Vector Machine, Urban classification, HYPXIM**

I. Introduction

This study aims at comparing the classification performances of up-to-date and coming space borne optical cameras on board a space platform over urban areas in the reflective domain (0.4 – 2.5 µm).

To this end, an airborne experiment over Toulouse (section 2) has been processed to simulate (section 3) synthetic space borne sensors: Pléiades, Sentinel-2 and HYPXIM. The corresponding images have then been used to evaluate the classification performance of each sensor over urban area (section 4).

II. Data description

Between the 23rd and the 25th of October 2012 the UMBRA campaign was carried out over the city of Toulouse (France) [1]. Different ground and airborne data were acquired during the campaign. In this study we used the airborne imagery to obtain the classification maps.

A. Study area

Toulouse (43°36′19″N 1°26′34″E) is a city in the South-West of France. Different housing density areas are found in the city. We have selected two different zones. First, a high housing density area in the city centre (hereafter City centre). Second, a low density housing area, placed in the Montaudran site (hereafter Montaudran), which main feature is an ancient landing strip. The Montaudran site is of interest because a urban development project is planned, so the classification of the present materials would be useful to detect future land cover changes.

B. Airborne data

During the UMBRA campaign, hyperspectral airborne acquisitions were done with the HySpex instrument (http://www.hyspex.no/). The instrument has two cameras: the Visible and Near Infrared (VNIR) one (160 bands from 0.4 µm to 1.0 µm, with a Full Width at Half Maximum, FWHM, of 3.6 nm) and the Shortwave Infrared (SWIR) one (256 bands from 1.0 µm to 2.5 µm, with a FWHM of 6.0 nm). VNIR and SWIR bands were georeferenced and registrated, with a ground sample distance (GSD) of 1.6 m.

III. Methodology

The geometrically corrected VNIR-SWIR image was used to simulate different spatial and spectral resolutions, corresponding to three real instruments. Finally, a technique of classification was applied to each simulated image. In the following lines we explain each methodological step in detail.

A. Instruments simulation

Three current instruments were chosen: the operative PLEIADES instrument (http://smsc.cnes.fr/PLEIADES/), the SENTINEL-2 instrument (https://earth.esa.int/) to be launched in 2015 and the HYPXIM sensor [2], which is under study. As a first step, just the spectral configurations were taken into account. Secondly, both, spectral and spatial features were considered. With all this, five cases of study are considered and introduced in the following lines: PLEIADES_1.6m, SENTINEL2_1.6m, SENTINEL2_9.6m, Hyper_1.6m and Hyper_8m.

The spectral configurations were obtained, for each central

R. Oltra-Carrió is with the ONERA, The French Aerospace Lab, Toulouse, 31055 France (e-mail: rosa.oltra_carrio@ onera.fr).

X. Briottet is with the ONERA, The French Aerospace Lab, Toulouse, BP 31055 France (e-mail: xavier.briottet@ onera.fr).

M. Bonhomme is with the École Nationale Supérieure d'Architecture de Toulouse, Laboratoire de Recherche en Architecture, Toulouse, 31106 France (e-mail: marion.bonhomme@toulouse.archi.fr).

wavelength, by averaging the spectral radiances over the bandwidth of the simulated sensor. For the GSD, an aggregation process was applied on the 1.6 m GSD HySpex radiance image ($L_{1.6m}$). As proposed in (1), the new aggregated radiances (L_{Xm}), at a GSD of Xm, were obtained by averaging all the N pixels values that contributed to the output pixel. Notice that X can only be proportional to 1.6 m.

$$L_{Xm} = \frac{1}{N}\sum_{i=1}^{N} L_{1.6m} \quad (1)$$

1) PLEIADES

The Pleiades system is developed by the *Centre National d'Etudes Spatiales* (CNES). It is composed by a panchromatic band (GSD: 0.7m) and 4 bands in the VNIR (GSD: 2.8m, bandwidth of 0.12 µm for bands B, G, R and of 0.2 µm for band NIR). The Panchromatic band is not used in this study. The PLEIADES simulated product, with 4 spectral bands and a GSD of 1.6 m is hereafter named PLEIADES_1.6m.

2) SENTINEL 2

The Sentinel 2 European Space Agency's mission covers VNIR and SWIR regions within 13 spectral bands at different GSD and bandwidth. Two products were generated, both with 9 spectral bands (bands in atmospheric absorption regions were excluded), the first one at 1.6 m of GSD (SENTINEL2_1.6m) and the second one at 9.6 m of GSD (SENTINEL2_9.6m).

3) HYPXIM

The HYPXIM sensor is a future hyperspectral space borne instrument leaded by the CNES, with a GSD of 8 m in the VNIR-SWIR range and of 1.8 m in a panchromatic band. In this study we took advantage of the HySpex spectral configuration to simulate the HYPXIM maps. The atmospheric absorption regions were removed from the study and only 245 bands from the 416 available in HySpex were used. Two products were evaluated, one at 1.6 m of GSD (Hyper_1.6m) and the other one at 8 m of GSD (Hyper_8m)

B. Classification

The method chosen was the Support Vector Machine (SVM), which is a supervised method usually used in urban areas ([3], [4]). The classifications were performed using at-sensor radiance values (W m^{-2} sr^{-1} μm^{-1}).

In urban areas, different classification levels can be considered. According to [5] the first level is composed by 4 classes: built up, vegetation, non-urban bare surfaces and water bodies. In this study we aim to differentiate these 4 classes and make a more detailed classification of the built up area, differentiating between roof surface materials but without considering the intraclass variability. Overall, 8 land cover classes were defined by visual inspection using the RGB false colour image. Six classes appear in both study areas (*Transportation areas*, *Tile roof*, *Metallic roof*, *Other roof*, *Vegetation* and *Shadow*), while *Water* class was only identified for the city centre area and B*are soil* class was only present in the Montaudran area. The *Other roof* class corresponds to no metal or tile roofs, such as asphalt shingle or gravel roofs. The transportation areas include asphalt and concrete roads and parking lots.

A large number of training samples per class was selected over the airborne image at 1.6 m GSD to assure the accuracy of the classification and to obtain a valid number of samples at coarser spatial resolutions. Moreover, at 1.6 m, it is easy to assign a pixel to a land cover class, but the latter is harder at coarser spatial resolutions. Training samples for each class were selected from georeferenced regions of interest, so the same geographic regions were used for all the spatial configurations. Despite of the effort made to assign pixels far from the boundary between different land covers; some mixed pixels were expected at coarser resolutions, due to the aggregation process and the large variability of urban materials in a low spatial scale. The spectral separability of each class was computed with the Jeffries-Matusita distance [6].

A dataset of reference pixels, or ground pixels, was selected. These pixels were independent from the training pixels and they were chosen following the same procedure: they were selected from the 1.6 m GSD image and then geolocated over the other GSD images. The classification accuracy was analyzed using the kappa coefficient (κ) and the overall accuracy. The kappa coefficient ranges between 0 (worst case) to 1 (best case: agreement for all the pixels between its assigned class and its ground truth class). The overall accuracy is measured as the relation between the number of well classified pixels and the total number of validation pixels (in %).

IV. Results

The results are divided in two sections, one for the city centre area and the other one for the Montaudran site.

A. City centre

Table I shows the performance results for the city centre case. Best results were obtained with the high spatial resolution images. SENTINEL2_1.6m map and Hyper_1.6m had equivalent results, which were better than the PLEIADES_1.6m performance. This result reveals the contribution of the SWIR bands to improve classification results.

For the case under study, the SWIR bands help to differentiate between the *Other roof class* and the *Transportation areas class*. Indeed, the Jeffries-Matusita distance between both land covers was near 1.9 for the Hyper_1.6m and SENTINEL2_1.6m cases but 1.3 for the PLEIADES_1.6m. Fig. 1 illustrates this behavior, we observe that Hyper_1.6m and SENTINEL2_1.6m images discriminated the asphalt of the roads while the PLEIADES_1.6m classified it as *Other roof*.

At coarser spatial resolutions, the hyperspectral imagery performs better than the multispectral one and similar than the PLEIADES_1.6m configuration. In Fig. 2 we observe that in Hyper_8m and SENTINEL2_9.6m maps a lot of details were lost. In Fig. 2 b and c we do not distinguish the street pattern,

but a mix of *Transportation areas*, *Tile roof*, *Other roof* and *Shadow pixels*.

B. Montaudran

The accuracy parameters obtained for the Montaudran site (Table I) are harder to understand than the city centre ones. The most accurate map is the Hyper_1.6m, the second one is the SENTINEL2_9.6m case and then all the other configurations have similar values of kappa coefficient (0.67), and overall accuracy, around 72%.

The presence of the old landing strip in the studied area (Fig. 3.d) plays an important role in the classification results. The pavement of this infrastructure is deteriorated and its spectral response is far from the asphalt roads which are currently in use. Even if the training samples over the highway and over the landing strip were associated to the *Transportation areas* class, both materials are so different that the SVM rule associated the first to the *Other roof* class and a lot of pixels of the latter to *Bare soil* class. This can be observed in Fig. 3 where the airdrome landing way appears in the center of the image and the highway is on its left. Another remarkable result from Fig. 3 is the presence of *Tile roof* in the PLEIADES_1.6m configuration, were *Vegetation* class was expected.

The success of the SENTINEL2_9.6m classification, compared to the results obtained with the SENTINEL2_1.6m image, could be explained by the aggregation process. Over the runway, pixels that were classified as *Bare soil* in the map at 1.6 m were classified as *Transportation areas* in the 9.6 m map, in accordance with the validation database. This is also the case for some pixels of the highway, while in the SENTINEL2_1.6m map they were classified as *Other roof*, in the SENTINEL2_9.6m map they were placed in the correct *Transportation area* class. Nevertheless, the decrease of resolution brings with it a loss of the detail of the urban map and narrow roads disappeared in the SENTINEL2_9.6m classification map.

Finally, we are going to observe some details of Hyper_8m and SENTINEL2_9.6m maps in Fig. 4, two main differences can be noted. First, in the top of the image there are new buildings which roofs and shadows were better characterized in the image Hyper_8m, while in the other case most of the pixels were classified as *Transportation areas* and the outlines of the buildings were hardly drawn by the shadow. Second, around the airfield, *Bare soil* pixels were identified in the Hyper_8m case, where *Vegetation* was expected, while in the SENTINEL2_9.6m case some *Tile roof* pixels appeared.

V. Conclusions

Two different housing density areas in the city of Toulouse were chosen to apply a supervised SVM classification method: the city centre area and the Montaudran site. Different spectral and spatial configurations, corresponding to real sensors were tested.

For both sites we realised that VNIR information was not sufficient to characterize urban materials. Therefore, the SWIR spectral range was essential to differentiate between classes. In the city centre area, performance of the multispectral SENTINEL2_1.6m map was similar to the performance of the hyperspectral case at the same spatial resolution. Nevertheless, the latter gave the best performances in the Montaudran site.

Results emphasize the need to introduce higher level of classes, such as different types of surfaces inside the *Transportation areas* class. In this context, the contribution of the hyperspectral signal should be studied and better results than in the multispectral case are expected. At lower spatial resolutions, correct results of accuracy were obtained: overall accuracy better than 70 % and kappa coefficient around 0.7. Nevertheless, 8 m and 9.6 m of GSD were too coarse to identify urban patterns and details, such as narrow streets. Comparing PLEIADES_1.6m and Hyper_8m maps, similar performances are noted. So, in urban areas, it seems that a coarse resolution of the hyperspectral sensor is partially compensated by its spectral richness. With the HYPXIM sensor, both requirements, high spatial and spectral resolution, may be achieved by the fusion of its panchromatic image (1.8 m of GSD) with its hyperspectral bands. Future works will be devoted to evaluate the benefit of this fusion in the classification performance.

References

[1] K. Adeline, A. Le Bris, F. Coubard, X. Briottet, N. Paparoditis, F. Viallefond, N. Rivière, J.P. Papelard, P. Deliot, J. Duffaut, S. Airault, N. David, G. Maillet, L. Poutier, P.Y. Foucher, V. Achard, J.P. Souchon, C. Thom. Description de la campagne aéroportée UMBRA : étude de l'impact anthropique sur les écosystèmes urbains et naturels avec de images THR multispectrales et hyperspectrales. *Revue Française de Photogrammétrie et de Télédétection*, 202, 2013.

[2] S. Michel, M.J. Lefevre-Fonollosa, S. Hosford. HYPXIM-A hyperspectral satellite defined for science, security and defense users. Hyperspectral Workshop, Frascati, Italy, ESA SP-683, (2010).

[3] M. Fauvel, J.A. Benedictsson, J. Chanussot, J.R. Sveinsson. Spectral and spatial classification of hyperspectrral data using SVMs and morphological profiles. *IEEE Transactions on Geoscience and Remote Sensing*, 46, 11, 3804:3814, (2004).

[4] X. Cao, J. Chen, H. Imura, O. Higashi. A SVM-based method to extract urban areas from DMSP-OLS and SPOT VGT data. *Remote Sensing of Environment*, 113, 2205:2209, (2009)

[5] M. Herold, M.E. Gardner, D.A. Roberts. Spectral resolution requirements for mapping urban areas. *IEEE Transactions on Geoscience and Remote Sensing*, 41, 1907:1919 (2003)

[6] J.A. Richards, X. Jia. Remote Sensing Digital Image Analysis. *Springer-Verlag*, Berlin, 4th edition, (2006).

TABLE I
ACCURACY COEFFICIENTS FROM THE SVM CLASSIFICATION

	City centre		Montaudran	
Name	Kappa coefficient	Overall accuracy (%)	Kappa coefficient	Overall accuracy (%)
PLEIADES_1.6m	0.80	82.6	0.67	71.6
SENTINEL2_1.6m	0.88	89.7	0.67	72.0
Hyper_1.6m	0.86	87.9	0.74	77.5
SENTINEL2_9.6m	0.66	71.4	0.71	75.9
Hyper_8m	0.77	80.7	0.67	71.6

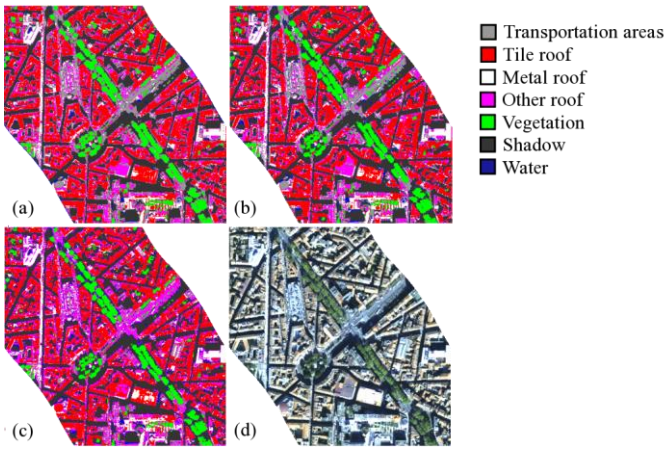

Fig. 1. SVM classification map using (a) Hyper_1.6m configuration; (b) SENTINEL2_1.6m configuration; and (c) PLEIADES_1.6m configuration. (d) Image of the area, RGB composition.

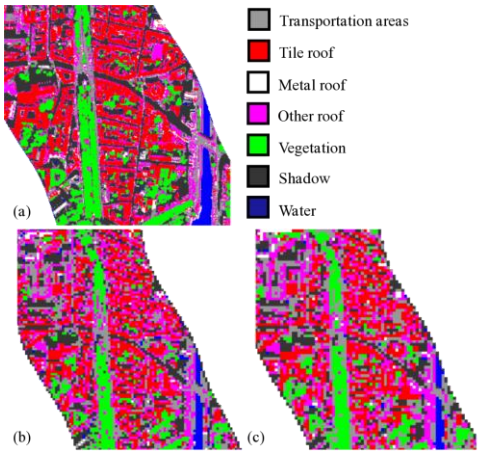

Fig. 2. SVM classification map using (a) Hyper_1.6m configuration; (a) Hyper_8m configuration; and (c) SENTINEL2_9.6m configuration.

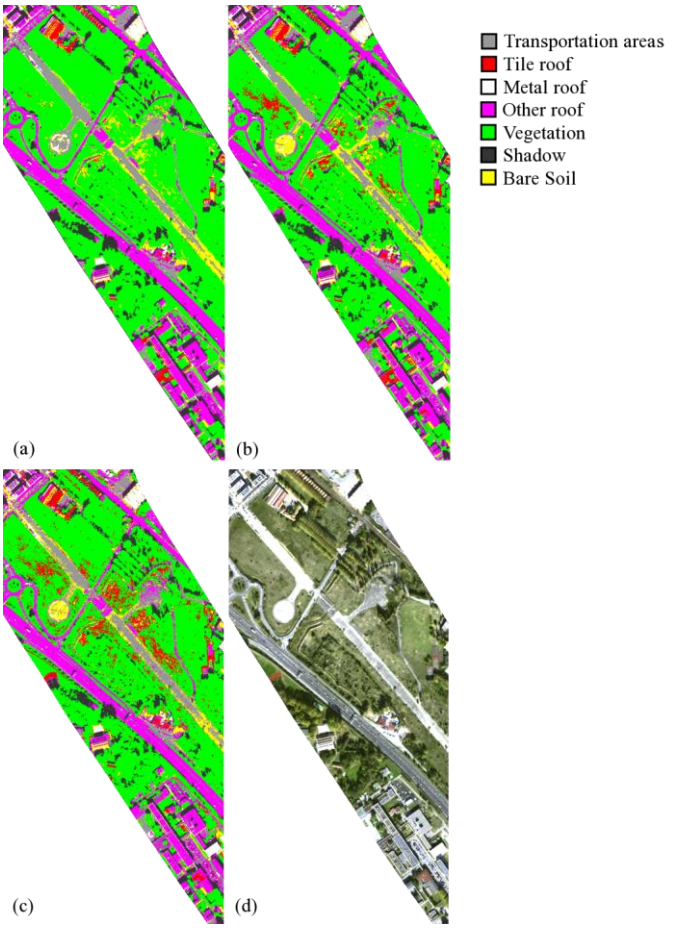

Fig. 3. SVM classification map using (a) Hyper_1.6m configuration; (b) SENTINEL2_1.6m configuration; and (c) PLEIADES_1.6m configuration. (d) Image of the area, RGB composition.

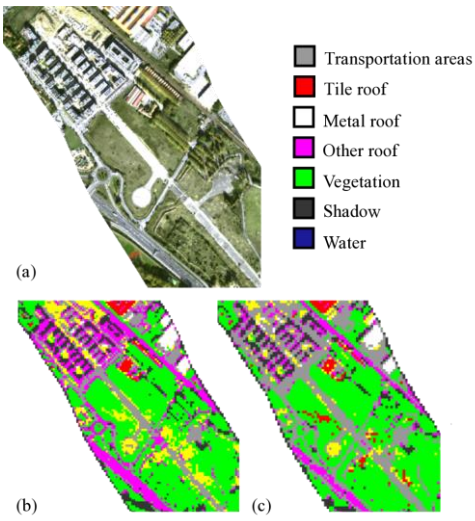

Fig. 4. (a) Image of the studied area, RGB composition. SVM classification map using (b) Hyper_8m configuration and (c) SENTINEL2_9.6m configuration.